Available online at www.sciencedirect.com
ScienceDirect
Catalysis Today 120 (2007) 240–244
CATALYSIS TODAY
www.elsevier.com/locate/cattod

Photo-oxidation mechanism of L-alanine in TiO_2 photocatalytic systems as studied by proton NMR spectroscopy

Masami Matsushita, Trung Huu Tran, Atsuko Y. Nosaka *, Yoshio Nosaka **

Department of Chemistry, Nagaoka University of Technology, Nagaoka 940-2188, Japan

Abstract

Photocatalytic decomposition of alanine as a representative amino acid was investigated in detail for nine different kinds of TiO_2 powders by proton NMR spectroscopy. Acetic acid was detected as a stable major intermediate via a fragile intermediate of acetaldehyde. Pyruvic acid was formed on rutile surface, while acetamide was detected on anatase surface. Pyruvic acid was formed directly from alanine, whereas acetamide was produced likely from acetaldehyde and ammonia, which are the decomposition components of alanine. In addition, small amount of formaldehyde and formic acid was formed and decomposing to CO_2.

Keywords: Photocatalyst; Titanium dioxide; Alanine; Rutile; Anatase; Amino acids; Decomposition; Reaction mechanism

1. Introduction

TiO_2 photocatalyst has been extensively investigated because of the properties such as strong oxidation power, chemical inertness, and detoxification, which are practically utilized in the environmental and industrial fields [1–5]. Although the number of the biochemical applications of TiO_2 mediated photo-oxidations is limited so far, the potential applications to the elimination of microorganisms, such as bacteria, fungi, mold, and virus is acknowledged. Actually *in vivo* the suppression of cancer cells by illuminated titania systems has been attempted [6]. To develop such applications effectively, a better understanding in degradation procedures of the elemental constituents of biological systems on photocatalysis would be invaluable. From this viewpoint we tried to investigate the photoinduced degradation mechanism of amino acids in TiO_2 photocatalytic systems by quantitative determination of the products with proton NMR spectroscopy, which has an advantage to obtain the direct information about the structures of the photo degradation species.

A large number of works of amino acids on TiO_2 have been published so far; for example Refs. [7–12]. For 20 amino acids, the decomposition has been analyzed by measuring the final products, such as NH_4^+, NO_3^-, and CO_2 [7]. By detecting initial decomposition step, this would assist in the understanding of the deterioration of biological functions which has not been elucidated so far. In the present study, as a first step, L-α-alanine was employed as an amino acid and the decomposition procedures were analyzed for various kinds of TiO_2 photocatalysts with different characteristics.

2. Experimental

The TiO_2 powders used were, Degussa P25 (Japan Aerosil), Hombikat UV-100 (Sachtleben Chemie), ST-01, ST-21 and PT-101 (Ishihara Techno), F4 (Showa Titanium), and AMT-100, AMT-600, and MT-500B (Tayca). In order to know the primary particle size and the crystalline composition of these powders, X-ray diffraction (XRD) of the TiO_2 powders was measured with a MacScience M03XHF22. The surface area was measured by the BET method with a Micromesotechs flowsorb (Shimadzu, 2300) with N_2 as the adsorbate. Anatase content and primary particle size, and BET surface areas of these TiO_2 powders are listed in Table 1.

L-Alanine was purchased from Wako Ltd. Pyruvic acid, acetic acid, acetamide, formaldehyde, methylamine, acetone, methylamine hydrochloride, *N*-methyl hydroxylamine hydrochloride (Nacalai Chemicals Ltd.), acetaldoxime, glycolic acid, and *N*-methylacetamide (Tokyo Kasei Inc.) were guaranteed

---

* Corresponding author.
** Corresponding author. Tel.: +81 258479315; fax: +81 258479315.
E-mail address: nosaka@nagaokaut.ac.jp (Y. Nosaka).

0920-5861/$ – see front matter © 2006 Elsevier B.V. All rights reserved.
doi:10.1016/j.cattod.2006.07.046

Table 1
Properties of TiO_2 photocatalyst powders used and the decomposition and formation rates in photocatalytic decomposition of alanine in aqueous suspension

Name of TiO_2	Anatase content (%)	Primary particle size (nm)	Secondary particle size (μm)	BET surface area ($m^2 g^{-1}$)	Adsorbed alanine (mM)[a]	Time profiles	Decomposition rate (μM/min) of alanine	Formation rate (μM/min)			
								Acetaldehyde	Acetic acid	Pyruvic acid	Acetamide
AMT-100	100	6	10.6	256	0.80	Fig. 3(A)	20.4	4.2	16.1	0.09	0.25
ST-01	100	8	15.3	295	0.66	Fig. 4(△)	15.0	2.2	6.3	0.10	0.26
UV-100	100	11	11.7	264	0.86	Fig. 4(□)	13.0	3.4	4.7	0.11	0.19
ST-21	100	21	18.5	62	0.52	Fig. 4(▽)	14.4	2.7	8.5	0.11	0.24
F4	88	29	0.26	53	1.10	Fig. 4(●)	10.4	4.1	4.4	0.10	0.35
AMT-600	100	30	13.5	50	0.74	Fig. 4(○)	24.6	6.5	8.0	0.14	0.20
P25	80	32	1.10	49	1.00	Fig. 4(▲)	13.8	4.0	3.8	0.15	0.24
MT-500B	0	36	21.6	43	0.45	Fig. 4(■)	6.4	1.8	2.4	0.45	0.09
PT-101	0	71	29.1	23	0.38	Fig. 3(B)	9.9	1.2	4.9	0.40	0.06

[a] Decreased concentration from 10 mM in 0.5 mL D_2O with 1 mg TiO_2.

reagents. Lactic acid (Junsei Chemical Co. Ltd.) was of extra pure grade.

^1H NMR measurements were carried out in a 5 mm o.d. NMR sample tube with a JEOL JNM-GX270 FT-NMR spectrometer at 270 MHz. 3-(Trimethylsilyl) propionate (TSP) was used as a standard for chemical shift, unless otherwise stated.

L-alanine was dissolved into D_2O (99.9% Isotec Inc.) containing 1 mg of TiO_2. Final pH and concentration were 5.6 ± 0.3 and 10 mM, respectively. The solution was UV irradiated with a 500 W high-pressure Hg lamp (USHIO, USH-500D) through Pyrex glass (>320 nm) under aerated conditions by rotating at room temperature outside the NMR spectrometer.

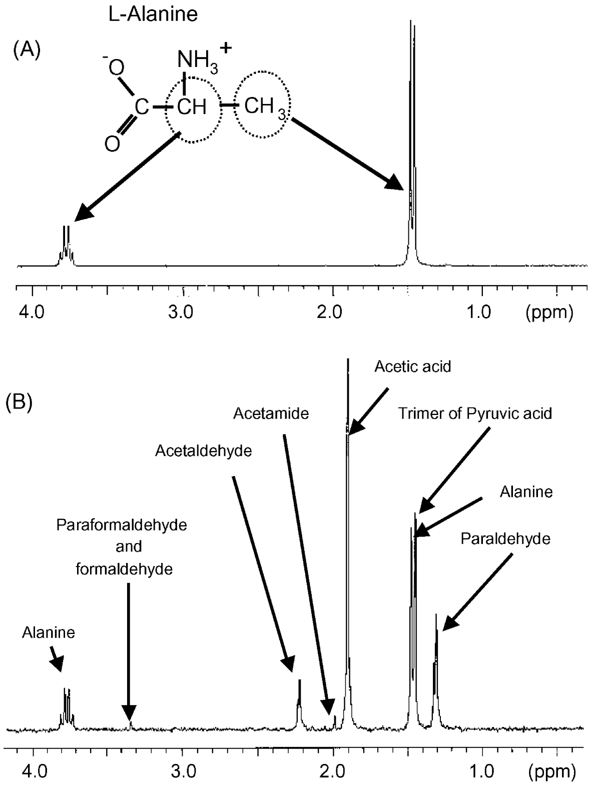

Fig. 1. (A) ^1H NMR spectrum of 10 mM L-alanine dissolved in D_2O measured at room temperature. (B) ^1H NMR spectrum of 10 mM L-alanine dissolved in D_2O with 1 mg of TiO_2 (AMT-100) measured at room temperature after UV irradiation for 10 h.

3. Results and discussion

The proton NMR spectrum of L-alanine in D_2O is shown in Fig. 1(A). The chemical shift and line width of α proton (3.78 ppm, 4.67 Hz) and methyl proton (1.48 ppm, 2.03 Hz) signals barely changed on addition of 1 mg TiO_2. In fact, all nine TiO_2 photocatalysts (P25, UV-100, ST-01, ST-21, F4, AMT-600 and MT-500B) displayed almost the same spectral features.

Upon UV irradiation with a decrease of the peak intensities of L-alanine signals, several photo-decomposition species appeared. Without photocatalytic powders no change in NMR spectrum of L-alanine was observed, indicating the reaction proceeded from photocatalytic reaction of TiO_2. Comparing the chemical shifts, coupling constants, and coupling patterns with those of the authentic reagents could assign most of the peaks as shown in Fig. 1(B). Spectra (A) and (B) in Fig. 2 shows the intermediate products detected for anatase and rutile TiO_2 powders, respectively. Besides the main components of acetic acid, acetaldehyde, paraldehyde, small amount of pyruvic acid, trimer of pyruvic acid, acetamide,

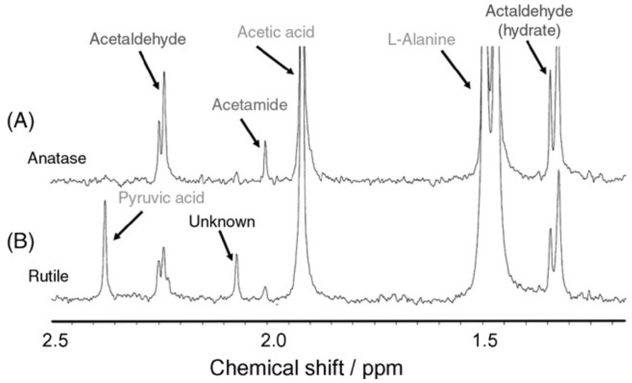

Fig. 2. A part of NMR spectra of the reaction products for photocatalysts with different crystal forms: (A) AMT-100 (anatase) and (B) PT-101 (rutile) after UV irradiation for 6 h.

Table 2
Assignments of observed ^{1}H NMR peaks for photocatalytic decomposition of alanine

Chemical shift (ppm)	Compounds
1.48 and 3.78	Alanine
1.33 and 5.25	Paraldehyde
1.47	Trimer of pyruvic acid
1.92	Acetic acid
2.01	Acetamide
2.06	Unknown
2.37	Pyruvic acid
2.24 and 9.67	Acetaldehyde
3.15	(Para)formaldehyde
8.45	Formic acid

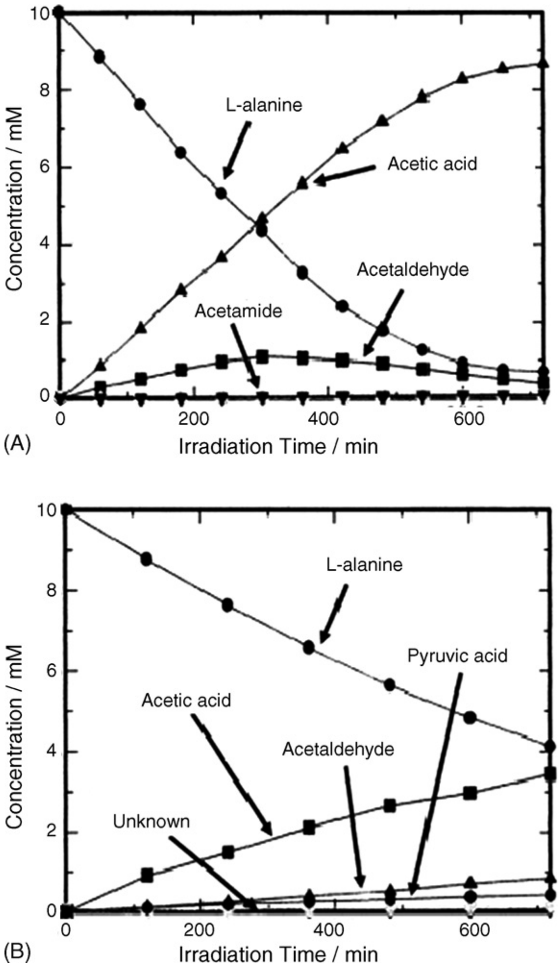

Fig. 3. The time profiles of the photocatalytic decomposition of L-alanine, and the formation of intermediates, acetic acid, acetaldehyde, pyruvic acid, acetamide, and unknown species for different TiO_2: (A) AMT-100 (anatase) and (B) PT-101 (rutile).

formaldehyde, and formic acid were identified as listed in Table 2. The chemical species showing the proton NMR peak at 2.06 ppm may have only one methyl group because of the chemical shift value. Plausible candidates for this signal were tested, but the following species were not the unknown species; methylamine, methanol, acetone, *N*-methyl hydroxylamine, acetaldoxime, glycolic acid, *N*-methylacetamide, lactic acid. Thus, at the present stage, this proton signal has not been assigned yet. Acetaldehyde is hydrated to form paraldehyde in water and they are equilibrated. As for acetaldehyde, the sum of the peak intensities for acetaldehyde and paraldehyde was accounted as acetaldehyde. It is notable that for anatase photocatalysts acetamide was observed, while for rutile photocatalysts pyruvic acid was observed instead.

Fig. 3 shows the time profile of L-alanine concentration and the intermediates formed in D_2O containing 1 mg of TiO_2 against the UV irradiation time for anatase TiO_2 (AMT-100) and rutile TiO_2 (PT-101). Fig. 4 shows the time profiles of the decomposed products for AMT-600, ST-01, ST-21, P25, F4, UV-100, and MT-500B. For these nine photocatalysts, the decomposition rate of L-alanine and the formation rates of the intermediate products were listed in Table 1.

The initial decomposition rates for rutile TiO_2 (MT-500B and PT-101) were smaller than those of other photocatalysts. Less adsorbability of alanine on rutile surface may be responsible for the reduced photocatalytic ability. However, some of anatase powders like UV-100 with high adsorption ability neither showed large initial decomposition rates. On the other hand the photocatalysts showing high decomposition rate, AMT-600 and AMT-100 did not show higher adsorbability. Therefore, the characteristics of TiO_2 such as secondary particle size that affects on the adsorbability would not be the main factor affecting the decomposition of alanine. For TiO_2 samples those presented high decomposition rate, the decomposition profiles of L-alanine in Fig. 4 were almost linear down to 3 mM, indicating that the reaction rate is not governed by the materials transfer but rather by the rate of the light absorption. Therefore the difference in the surface reaction rates among the deferent photocatalysts barely reflects the present initial decomposition rates. The growth rates of acetamide listed in Table 1 were almost proportional to the decomposition rates of alanine, indicating the decomposition rate determines the formation rate of acetamide. The high formation rate of acetic acid for AMT-100 may be caused by the slow decomposition rate of acetic acid by this particular photocatalyst.

As presented in Fig. 3(A), the concentration of acetaldehyde showed a maximum at the crossing point of the decay of alanine and the growth of acetic acid and the total concentration of these three compounds was almost constant during the reaction. This feature in the time profile implies that the main decomposition route is the consecutive reaction from alanine to acetic acid via acetaldehyde, though the reaction rates varied for the different photocatalysts:

$$\text{alanine} \xrightarrow{k_1} \text{acetaldehyde} \xrightarrow{k_2} \text{acetic acid}$$

Based on the kinetic analysis for the first order consecutive reaction, the concentration of intermediate molecule, acetaldehyde, at time *t* could be obtained by the following equation:

$$[\text{acetaldehyde}] = \frac{A_0 k_1 (\exp(-k_2 t) - \exp(-k_1 t))}{k_1 - k_2}$$

where A_0 represents the initial concentration of alanine, i.e., 10 mM. From the concentration of acetaldehyde and the time at the maximum concentration, the apparent reaction rate

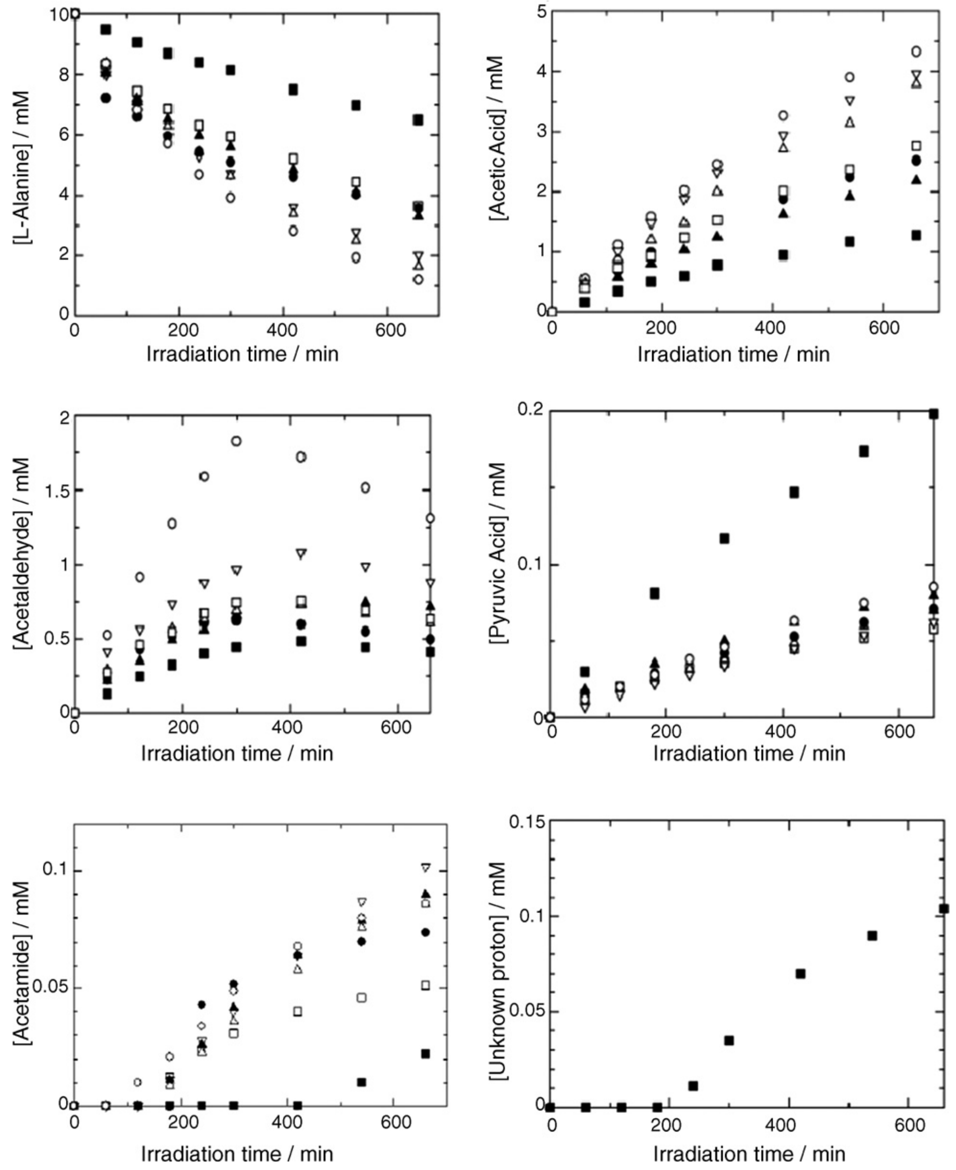

Fig. 4. The time profiles for the decomposition of L-alanine and the formation of acetic acid, acetaldehyde, pyruvic acid, and acetamide, by using various photocatalysts: (■) MT-500B; (□) UV-100; (●) F4; (▲) P25; (▽) ST-21; (△) ST-01; (○) AMT-600.

constants, k_1 and k_2, for this consecutive reaction were calculated to be 1.7×10^{-3} and 6×10^{-3} min^{-1} for AMT-600 (anatase), and 0.4×10^{-3} and 7×10^{-3} min^{-1} for MT-500B (rutile), respectively. The values of k_1 and k_2 for other TiO_2 are within these values. Thus, the apparent decomposition rate constant of acetaldehyde does not depend on the crystal form of the photocatalysts. This would mean that the reaction in the second step is so fast that the excitation rate of the photocatalyst fully determines the reaction rate.

On the other hand, the dependence of the crystal structure was clearly reflected in the formation rate of pyruvic acids and acetamide. For rutile TiO_2 MT-500B, significant amount of pyruvic acid was formed. For the mixture of anatase and rutile, P25 (20% of rutile content) the amount was similar to those for the 100% anatase. However, when P25 was irradiated at the wavelength larger than 400 nm, where mainly rutile powder of P25 could be excited, the amount of the produced pyruvic acid was substantially increased. Pyruvic acid was produced without an induction period, which indicates that pyruvic acid was produced directly from alanine at a certain active sites on rutile surface. On rutile surface the formation of oxygen molecules from water via hydroperoxo has been reported [13]. The selective formation of pyruvic acid on rutile surface may correlate with this property of the rutile surface.

Acetamide was formed preferably on anatase TiO_2 after certain induction period. Then acetamide may be produced as a byproduct in the formation of acetic acid from acetalydehyde in the presence of ammonia, which is the decomposition product of alanine. Since hydrolysis of acetamide produces acetic acid and ammonium ion, the same reaction would take place in photocatalytic system. The unknown species showing the

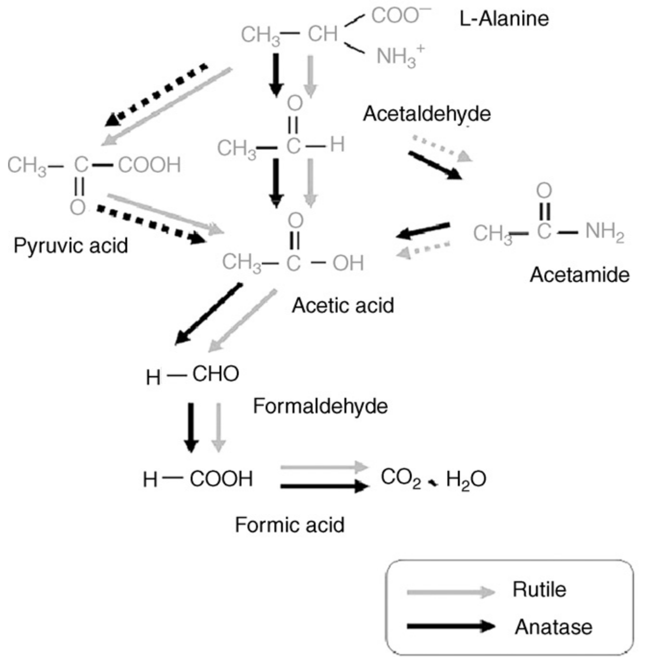

Fig. 5. Difference in the decomposition rout of L-alanine with photocatalysts of different crystal structures: anatase (black arrows) and rutile (gray arrows). Solid arrows shows a major reaction route, while dashed arrows represent a minor reaction route.

proton NMR peak at 2.06 ppm also has an induction period to be produced as shown in Fig. 4.

The photocatalytic decomposition routes deduced from the present observations are summarized and illustrated in Fig. 5. The only very small amount of formaldehyde and formic acid could be detected, suggesting the decomposition rates of these compounds are too fast as compared with that of acetic acid. Hidaka et al. [7] reported the photocatalytic degradation steps of 0.1 mM alanine based on the observations that the formation rate of CO_2 was almost equal to that of NH_4^+ besides the detection of peroxide intermediate by the potassium iodide procedure. Although they assumed many intermediate radical species, in the present work we could detect the presence of the stable intermediates by using NMR spectroscopy to clarify the degradation steps.

4. Summary

Photocatalytic decomposition of alanine as a representative amino acid was investigated in detail for nine different kinds of commercially available TiO_2 powders. The photocatalytic reaction has been performed in NMR sample tube and then, from NMR spectra recorded in the irradiation periods, the concentrations of the reactant and the intermediate products were measured. Acetic acid was detected as a stable major intermediate, which is produced via an intermediate of acetaldehyde. Pyruvic acid was formed on rutile surface, while acetamide was detected on anatase surface. Pyruvic acid was formed directly from alanine on rutile surface, on which the formation of hydroperoxo species has been reported. On the other hand, acetamide was produced likely from the reaction products, acetaldehyde and ammonia, because the formation needed some incubation time. Since the amount of formaldehyde and formic acid was very small, the photocatalytic decomposition of these intermediate was very fast.

Acknowledgements

This work was supported in part by a Grant-in-Aid on the Priority Area (417) and a 21st COE program from the Ministry of Education, Culture, Science and Technology (MEXT), Japan.

References

[1] A. Fujishima, K. Hashimoto, T. Watanabe, TiO_2 Photocatalysis: Fundamentals and Applications, BKC Publ., Tokyo, 1999.
[2] M. Kaneko, I. Ohkura (Eds.), Photocatalysis—Science and Technology, Kodansha-Springer, Tokyo, 2002.
[3] M.R. Hoffmann, S.T. Martin, W. Choi, D.W. Bahnemann, Chem. Rev. 95 (1995) 69.
[4] A. Mills, S.L. Hunte, J. Photochem. Photobiol. A 108 (1997) 1.
[5] A. Fujishima, T.N. Rao, D.A. Tryk, J. Photochem. Photobiol. C: Photochem. Rev. 1 (2000) 1.
[6] R. Cai, K. Hashimoto, A. Fujishima, J. Electroanal. Chem. 326 (1992) 345.
[7] H. Hidaka, S. Horikoshi, K. Ajisaka, J. Zhao, N. Serpone, J. Photochem. Photobiol. A 108 (1997) 197.
[8] H. Hidaka, K. Ajisaka, S. Horikoshi, T. Oyama, J.C. Zhao, N. Serpone, Catal. Lett. 60 (1999) 95.
[9] S. Ikeda, N. Sugiyama, B. Pal, G. Marci, L. Palmisano, H. Noguchi, K. Uosaki, B. Ohtani, Phys. Chem. Chem. Phys 3 (2001) 267.
[10] G. Martra, S. Horikoshi, M. Anpo, S. Coluccia, H. Hidaka, Res. Chem. Intermed. 28 (2002) 359.
[11] M.A. Strehle, P. Rosch, R. Petry, A. Hauck, R. Thull, W. Kiefer, J. Popp, Phys. Chem. Chem. Phys 6 (2004) 5232.
[12] Y.K. Takahara, Y. Hanada, T. Ohno, S. Ushiroda, S. Ikeda, M. Matsumura, J. Appl. Electrochem. 35 (2005) 793.
[13] R. Nakamura, Y. Nakato, J. Am. Chem. Soc. 126 (2004) 1290.